

Formation and Structures of Hafnocene Complexes in MAO- and $\text{AlBu}^i_3/\text{CPh}_3[\text{B}(\text{C}_6\text{F}_5)_4]$ -Activated Systems

Konstantin P. Bryliakov,^{*,†} Evgenii P. Talsi,[†] Alexander Z. Voskoboynikov,[‡]
Simon J. Lancaster,[§] and Manfred Bochmann^{*,§}

Boreshkov Institute of Catalysis, Siberian Branch of the Russian Academy of Sciences, 630090, Novosibirsk, Russian Federation, Department of Chemistry, Moscow State University, Lomonosovskiy Prospekt 1, 113000 Moscow, Russian Federation, and Wolfson Materials and Catalysis Centre, School of Chemical Sciences and Pharmacy, University of East Anglia, Norwich NR4 7TJ, United Kingdom

Received July 12, 2008

The formation of cationic species relevant to olefin polymerization based on (SBI)HfCl₂, Me₂C(C₅H₄)(Flu)HfCl₂, Ph₂C(C₅H₄)(Flu)HfCl₂, and L'HfCl₂ activated by MAO, AlMe₃/CPh₃[B(C₆F₅)₄], and AlBuⁱ₃/CPh₃[B(C₆F₅)₄] (SBI = *rac*-Me₂Si(Ind)₂; L' = C₂H₄(Flu)(5,6-C₃H₆-2-MeInd)) was studied by ¹H, ¹³C, and ¹⁹F NMR spectroscopy. Thermally stable heterobinuclear intermediates of the type [LHf(μ-Me)₂AlMe₂]⁺[MeMAO]⁻ and [LHf(μ-Me)₂AlMe₂]⁺[B(C₆F₅)₄]⁻ were identified when using MAO and AlMe₃/CPh₃[B(C₆F₅)₄] as activators, respectively. The stability of these species explains the low productivity of hafnocene catalysts in the presence of AlMe₃-containing activators, compared to zirconocenes. By contrast, in the ternary systems LHfCl₂/AlBuⁱ₃/CPh₃[B(C₆F₅)₄] hydride species were detected that must be responsible for the formation of the highly active sites in olefin polymerization. The ionic hydrido species differ significantly in stability. The formation of the mixed-alkyl complex L'Hf(Me)CH₂SiMe₃ proceeds with surprisingly high diastereoselectivity; the sterically more hindered isomer is produced preferentially. It reacts with CPh₃[B(C₆F₅)₄] to afford the ion pair [L'Hf-CH₂SiMe₃]⁺[B(C₆F₅)₄]⁻ as two diastereomers that exist in dynamic equilibrium. The rates of site epimerization of this ion pair indicate only small energy differences between the two isomers.

Introduction

In the past few years, interest in hafnium-based metallocene and post-metallocene olefin polymerization catalysts has risen sharply, resulting in promising new findings.^{1–6} It was shown that ultrahigh molecular weight polypropylene elastomers could be prepared using highly active C₁-symmetric hafnocene catalysts.^{1–3} Pyridyl-amide hafnium complexes were recently optimized for commercial high-temperature propylene polymerization.^{4–6} In addition, the latter catalysts have been applied in the high-volume preparation of olefin block copolymers through chain shuttling polymerization.⁷

Significantly, the aforementioned catalysts are effectively activated by mixtures of triisobutyl aluminum and cation-generating borates (e.g., AlBuⁱ₃/CPh₃[B(C₆F₅)₄]), whereas me-

thylalumoxane (MAO) appeared to be an unexpectedly poor activator.^{1–6} Similar differences in the catalytic productivity of AlBuⁱ₃/CPh₃[B(C₆F₅)₄]⁻ and MAO-activated systems were previously reported for some other C₁-, C₂-, and C_s-symmetric hafnocenes.^{8–10} Determining the origin of these differences is self-evidently an important task.

Previously, some of us have shown that heterobinuclear ion pairs [(SBI)Zr(μ-Me)₂AlMe₂]⁺[Me-MAO]⁻ are formed upon the activation of the C₂-symmetric zirconocene (SBI)ZrCl₂ (SBI = *rac*-Me₂Si(Ind)₂) with MAO,^{11,12} whereas in the ternary catalytic system (SBI)ZrCl₂/AlBuⁱ₃/[CPh₃][B(C₆F₅)₄] the last confidently assigned precursor of the active species of polymerization was the binuclear complex [(SBI)Zr(μ-Cl)₂Zr(SBI)][B(C₆F₅)₄]₂.¹³ In addition, at high Al/Zr ratios (≥20), the hydride- and allyl-bridged heterobinuclear complex [(SBI)Zr(μ-H)(μ-C₄H₇)-AlBuⁱ₂][B(C₆F₅)₄] was identified, which is probably the thermodynamic sink of this catalyst system.¹³ A similar hydride-

* Corresponding authors. (K.P.B.) Fax: +7 383 3308056. E-mail: bryliako@catalysis.ru. (M.B.) Fax: (+44) 1603 592044. E-mail: m.bochmann@uea.ac.uk.

[†] Boreshkov Institute of Catalysis.

[‡] Moscow State University.

[§] University of East Anglia.

- (1) Rieger, B.; Troll, C.; Preuschen, J. *Macromolecules* **2002**, *35*, 5742.
- (2) Hild, S.; Cobzaru, C.; Troll, C.; Rieger, B. *Macromol. Chem. Phys.* **2006**, *207*, 665.
- (3) Cobzaru, C.; Rieger, B. *Macromol. Symp.* **2006**, *236*, 151.
- (4) Boussie, T. R.; Diamond, G. M.; Goh, C.; Hall, K. A.; LaPointe, A. M.; Leclerc, M. K.; Murphy, V.; Shoemaker, J. A. W.; Turner, H.; Rosen, R. K.; Stevens, J. C.; Alfano, F.; Busico, V.; Cipullo, R.; Talarico, G. *Angew. Chem., Int. Ed.* **2006**, *45*, 3278.
- (5) Froese, R. D. J.; Hustad, P. D.; Kuhlman, R. L.; Wenzel, T. T. *J. Am. Chem. Soc.* **2007**, *129*, 7831.
- (6) Boussie, T. R.; Diamond, G. M.; Goh, C.; Hall, K. A.; LaPointe, A. M.; Leclerc, M. K.; Lund, C.; Murphy, V. U.S. Pat. 7.018.949, 2006.
- (7) Arriola, D. J.; Carnahan, E. M.; Hustad, P. D.; Kuhlman, R. L.; Wenzel, T. T. *Science* **2006**, *312*, 714.

(8) Seraidaris, T.; Kaminsky, W.; Seppälä, J.; Löfgren, B. *Macromol. Chem. Phys.* **2005**, *206*, 1319.

(9) Yano, A.; Sone, M.; Yamada, S.; Hasegawa, S.; Akimoto, A. *Macromol. Chem. Phys.* **1999**, *200*, 924.

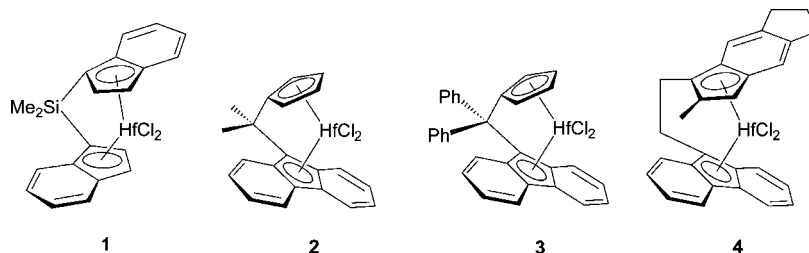
(10) Seraidaris, T.; Puranen, A.; Karessoja, M.; Löfgren, B.; Repo, T.; Leskelä, M.; Seppälä, J. *J. Polym. Sci. A: Polym. Chem.* **2006**, *44*, 4743.

(11) Bryliakov, K. P.; Semikolenova, N. V.; Yudaev, D. V.; Zakharov, V. A.; Brintzinger, H. H.; Ystenes, M.; Rytter, E.; Talsi, E. P. *J. Organomet. Chem.* **2003**, *683/1*, 92.

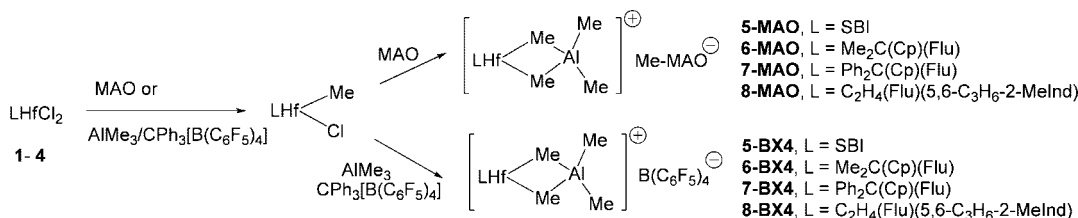
(12) For related studies on the zirconocene/MAO system see also: (a) Tritto, I.; Donetti, R.; Sacchi, M. C.; Locatelli, P.; Zannoni, G. *Macromolecules* **1997**, *30*, 1247. (b) Babushkin, D. E.; Semikolenova, N. V.; Zakharov, V. A.; Talsi, E. P. *Macromol. Chem. Phys.* **2000**, *201*, 558. (c) Babushkin, D.; Brintzinger, H. H. *J. Am. Chem. Soc.* **2002**, *124*, 12869. (d) Babushkin, D.; Brintzinger, H. H. *Chem. Eur. J.* **2007**, *13*, 5294.

(13) Bryliakov, K. P.; Talsi, E. P.; Semikolenova, N. V.; Zakharov, V. A.; Brand, J.; Alonso-Moreno, C.; Bochmann, M. *J. Organomet. Chem.* **2007**, *692*, 859.

Chart 1



Scheme 1



bridged complex was earlier observed by Götz and co-workers in the reaction of the *C*_s-symmetric Ph₂C(Cp)(Flu)ZrCl₂ with AlBuⁱ₃ and [PhNMe₂H][B(C₆F₅)₄].¹⁴

In this work, the structures of the cationic metallocene species formed upon activation of *C*₂-, *C*_s-, and *C*₁-symmetric hafnocenes **1–4** (Chart 1) with MAO and AlBuⁱ₃/CPh₃[B(C₆F₅)₄] were compared. Earlier studies on the use of Zr- and Hf-CH₂SiMe₃ complexes have established the role of this alkyl ligand as models for the metal-bound polymeryl chain and provided detailed information on the solution structure, ion aggregation, and dynamics of metallocene catalysts.^{15–17} We report here the synthesis of mixed-alkyl derivatives of the *C*₁-symmetric complex **4**, together with the ligand dynamics of the ion pair derived from this ligand system on activation with AlBuⁱ₃/CPh₃[B(C₆F₅)₄]. Under closely analogous conditions, hafnium was found to produce different resting states from zirconium.¹⁸

Results and Discussion

Activation of Hafnocene Dichlorides with MAO and AlMe₃/CPh₃[B(C₆F₅)₄]. On reacting (SBI)HfCl₂ (**1**) with an excess of MAO in toluene-*d*₈, two types of intermediates were identified. The first one, predominating at Al/Hf ratios of 30–60, was identified as (SBI)HfMeCl. The second one (**5-MAO**) becomes the predominant species at an Al/Hf ratio of ≥240. On the basis of its NMR data, **5-MAO** was identified as the heterobinuclear outer-sphere ion pair [(SBI)Hf(μ-Me)₂AlMe₂]⁺[MeMAO][−] (Scheme 1). This compound proved thermally stable at room temperature for at least 1 day. It showed quite low activity for ethylene polymerization; only traces of polyethylene were detected in the sample after injecting 9 equiv of ¹³C₂H₄ and storing at −10 °C for 2 h.

(14) Götz, C.; Rau, A.; Luft, G. *J. Mol. Catal. A: Chem.* **2002**, *184*, 95.

(15) Song, F.; Cannon, R. D.; Bochmann, M. *Chem. Commun.* **2004**, 542.

(16) Song, F.; Lancaster, S. J.; Cannon, R. D.; Schormann, M.; Humphrey, S.; Zuccaccia, C.; Macchioni, C.; Bochmann, M. *Organometallics* **2005**, *24*, 1315.

(17) (a) Alonso-Moreno, C.; Lancaster, S. J.; Zuccaccia, C.; Macchioni, A.; Bochmann, M. *J. Am. Chem. Soc.* **2007**, *127*, 9282. (b) Alonso-Moreno, C.; Lancaster, S. J.; Wright, J. A.; Hughes, D. L.; Zuccaccia, C.; Correa, A.; Macchioni, A.; Cavallo, L.; Bochmann, M. *Organometallics*, in press. (c) For DFT calculations on the ion pair [(SBI)Zr-CH₂SiMe₃]⁺[B(C₆F₅)₄][−] see: (d) Ducère, J. M.; Cavallo, L. *Organometallics* **2006**, *25*, 1431.

(18) For the reactions of Cp₂HfEt₂ with CPh₃[B(C₆F₅)₄] see: Bochmann, M.; Lancaster, S. J. *J. Organomet. Chem.* **1995**, *497*, 55.

For comparison, **1** was reacted with AlMe₃/CPh₃[B(C₆F₅)₄] (Hf:Al:B = 1:30:1.1) to give [(SBI)Hf(μ-Me)₂AlMe₂]⁺[B(C₆F₅)₄][−] (**5-BX₄**) (Scheme 1). **5-BX₄** is stable at room temperature for days. Addition of 3 equiv of propene to the [(SBI)Hf(μ-Me)₂AlMe₂]⁺[B(C₆F₅)₄][−] species at low temperature (−40 °C) resulted in no monomer incorporation or propene consumption. Warming the sample in 10 °C steps led to the disappearance of the propene signals only at +20 °C, the spectrum of **5-BX₄** remaining unchanged. Injection of 3 equiv of ¹³C₂H₄ into the sample containing [(SBI)Hf(μ-Me)₂AlMe₂]⁺[B(C₆F₅)₄][−] at −10 °C showed slow ethylene consumption at this temperature; there was complete ¹³C₂H₄ conversion within ca. 2 h. Again the spectrum of **5-BX₄** remained essentially unchanged, a typical behavior of these catalysts where the first insertion is rate limiting.^{19–21}

The *C*_s-symmetric complexes **2** and **3** react with MAO and AlMe₃/CPh₃[B(C₆F₅)₄] in a similar manner: the monomethylated derivatives Me₂C(Cp)(Flu)HfMeCl and Ph₂C(Cp)(Flu)HfMeCl were detected as the main species at Al_{MAO}:Hf ratios of 90:1, while increasing the Al_{MAO}:Hf ratio to 300:1 led to quantitative formation of [Me₂C(Cp)(Flu)Hf(μ-Me)₂AlMe₂]⁺[MeMAO][−] (**6-MAO**) and [Ph₂C(Cp)(Flu)Hf(μ-Me)₂AlMe₂]⁺[MeMAO][−] (**7-MAO**), respectively. Activation with AlMe₃/CPh₃[B(C₆F₅)₄] gave [Me₂C(Cp)(Flu)Hf(μ-Me)₂AlMe₂]⁺[B(C₆F₅)₄][−] (**6-BX₄**) and [Ph₂C(Cp)(Flu)Hf(μ-Me)₂AlMe₂]⁺[B(C₆F₅)₄][−] (**7-BX₄**). In these *C*_s-symmetric examples, the two terminal Al-Me groups are inequivalent. All these heterobinuclear intermediates are thermally stable for at least 1 day at room temperature.

The spectra of the *C*₁-symmetric complex **4** with MAO or AlMe₃/CPh₃[B(C₆F₅)₄] are more complicated. At Al/Hf ratios of 30–70, several (three or four) types of Hf complexes were found to coexist in comparable concentrations, whereas at Al/Hf ratios of 90:1 or higher, only one species, identified as [(L')Hf(μ-Me)₂AlMe₂]⁺[MeMAO][−] (**8-MAO**) (L' = C₂H₄(Flu)(5,6-C₃H₆-2-MeInd)), was found to prevail and appeared to be stable for days in an NMR tube at room temperature. The interaction

(19) Review: Bochmann, M. *J. Organomet. Chem.* **2004**, *689*, 3982.

(20) Bochmann, M.; Jaggar, A. J.; Nicholls, J. C. *Angew. Chem., Int. Ed. Engl.* **1990**, *29*, 780.

(21) (a) Fink, G.; Zoller, W. *Makromol. Chem.* **1981**, *182*, 3265. (b) Fink, G.; Rottler, R. *Angew. Makromol. Chem.* **1981**, *94*, 25. (c) Fink, G.; Schnell, D. *Angew. Makromol. Chem.* **1982**, *105*, 31. (d) Mynott, R.; Fink, G.; Fenzl, W. *Angew. Makromol. Chem.* **1987**, *154*, 1. (e) Fink, G.; Fenzl, W.; Mynott, R. *Z. Naturforsch. Teil B* **1985**, *40b*, 158.

of **4** with $\text{AlMe}_3/\text{CPh}_3[\text{B}(\text{C}_6\text{F}_5)_4]$ (Hf:Al:B = 1:50:1.1) resulted in the formation of a brown oil containing cationic species identified as $[\text{L}^i\text{Hf}(\mu\text{-Me})_2\text{AlMe}_2]^+[\text{B}(\text{C}_6\text{F}_5)_4]^-$ (**8-BX₄**). The C_1 symmetry of **8-MAO** is reflected in the four separate ^1H NMR signals seen for the bridging and terminal Al-Me groups.

Raising the temperature leads to the coalescence of the ^1H peaks of the terminal AlMe_2 groups (at 343 K, apparent $\Delta G_{\text{ex}} = 17.5 \text{ kcal mol}^{-1}$), the bridging methyls remaining nonequivalent (see Supporting Information). It is poorly reactive toward propene: when ca. 3.5 equiv of propene was added to the solution of **8-BX₄** at low temperature, complete consumption was achieved only after warming the sample above +20 °C.

The results confirm that the alkylation of hafnocenes with AlMe_3 proceeds in stages, first forming the monomethyl chloride, followed by dechlorination and formation of the heterobinuclear cation $[\text{LHf}(\mu\text{-Me})_2\text{AlMe}_2]^+$. We note that higher $\text{Al}_{\text{MAO}}:\text{Hf}$ ratios are generally needed for complete conversion of *ansa*-hafnocenes to $[\text{LHf}(\mu\text{-Me})_2\text{AlMe}_2]^+[\text{MeMAO}]^-$ (up to 240–300) than in the cases of *ansa*-zirconocenes¹¹ and *ansa*-titanocenes,²² where $\text{Al}_{\text{MAO}}:\text{metal}$ ratios of 100–200 were enough for complete conversion to the heterobinuclear species. The Hf ion pairs are poorly active in ethylene and propene polymerization. This is not unexpected taking into account the observed low productivity of the *ansa*-hafnocene/MAO systems in catalytic olefin polymerizations.^{1–6,23,24}

Activation of (SBI)HfCl₂ with $\text{AlBu}^i_3/\text{CPh}_3[\text{B}(\text{C}_6\text{F}_5)_4]$. Most highly active borate-activated metallocene systems involve AlBu^i_3 as a component. It is therefore important to understand the nature of the active sites formed in the systems hafnocene/ $\text{AlBu}^i_3/\text{CPh}_3[\text{B}(\text{C}_6\text{F}_5)_4]$ and thus answer the question of why activation with $\text{AlBu}^i_3/\text{CPh}_3[\text{B}(\text{C}_6\text{F}_5)_4]$ leads to much more productive catalysts than MAO. To this end, the reactions of **1–4** with AlBu^i_3 in the presence and absence of $\text{CPh}_3[\text{B}(\text{C}_6\text{F}_5)_4]$ were studied by ^1H and ^{13}C NMR spectroscopy.

Initially the alkylation of **1** with AlBu^i_3 in the absence of trityl salt was probed. At room temperature, the monoalkylation equilibrium is established within 5 min, a 30-fold excess of AlBu^i_3 leading to a 2:3 mixture of (SBI)HfCl₂ and (SBI)Hf-(Buⁱ)Cl. One can see that (SBI)HfCl₂ requires a much higher Al:metal ratio for monoalkylation than (SBI)ZrCl₂ (for the latter, 5 equiv of AlBu^i_3 gave 90% monoalkyl product).¹³ That is why relatively high Al:Hf ratios (generally 30–50 and 10 in some cases) were used in subsequent experiments.

The reaction of **1** with $\text{AlBu}^i_3/\text{CPh}_3[\text{B}(\text{C}_6\text{F}_5)_4]$ (Hf:Al:B = 1:10–50:1.1) gave a red oil, which precipitated to the bottom of the NMR tube. The upper (toluene) phase was removed; its ^1H NMR spectrum showed the formation of Ph_3CH along with isobutene in the course of activation of **1**. The oily phase was dissolved in a mixture of toluene-*d*₈ and 1,2-difluorobenzene (5:1 v/v), and the NMR spectra of the resulting samples were measured. Only one species (**9**) was found to prevail in solution over a broad range of Al:Hf ratios (10–50:1). Compound **9** was stable at room temperature for hours, and complete degradation took place only on heating to +95 °C.

The ^1H NMR spectrum is shown in Figure 1. According to the ^{13}C NMR spectra of **9**, Hf-CH₂- groups were absent. However, there are two hydride signals marked as H¹ (1H, t, $^2J_{\text{HH}} = 5 \text{ Hz}$) and H² (2H, d, $^2J_{\text{HH}} = 5 \text{ Hz}$), which display correlation peaks in the ^1H COSY spectra. On the basis of this information, **9** is formulated as a hydride-bridged binuclear species, $[(\text{SBI})\text{Hf}(\mu\text{-H})_2\text{Al}(\text{H})\text{Bu}^i]^+[\text{B}(\text{C}_6\text{F}_5)_4]^-$ (Scheme 2).

The facile formation of hydrido-bridged species on activation of hafnocene dichlorides with $\text{AlBu}^i_3/\text{CPh}_3[\text{B}(\text{C}_6\text{F}_5)_4]$ is in contrast to the reaction of related zirconocenes with AlBu^i_3 -enriched MAO, which produces predominantly methyl-bridged complexes of the type $[(\text{SBI})\text{Zr}(\mu\text{-Me})_2\text{Al}(\text{R})\text{Bu}^i]^+$ (R = Me, Buⁱ), whereas hydride-bridged products are only barely detectable at elevated $\text{AlBu}^i_3/\text{Zr}$ ratios.^{12d} By contrast, the addition of HAlBu^i_2 to $[(\text{L})\text{Zr}(\mu\text{-Me})\text{AlMe}_2]^+[\text{Me-MAO}]^-$ was found to lead to the formation of neutral zirconocene hydrides $\text{LZrH}_2 \cdot n(\text{AIR}_2\text{X})$.²⁵

We had found earlier that zirconocenes react with $\text{AlBu}^i_3/\text{CPh}_3[\text{B}(\text{C}_6\text{F}_5)_4]$ in several steps to give eventually a hydrido species, $[(\text{SBI})\text{Zr}(\mu\text{-H})(\mu\text{-C}_4\text{H}_7)\text{AlBu}^i_2][\text{B}(\text{C}_6\text{F}_5)_4]$, a likely thermodynamic sink.¹³ The reactivity of **9** toward olefins was therefore tested to probe its ability to act as direct catalyst precursor. The $\mu\text{-H}$ product **9** is certainly more reactive than the $\mu\text{-Me}$ compound **5-BX₄**, and 3 equiv of propene added at –30 °C was rapidly consumed on warming to 0 °C, although the ^1H NMR spectrum of the hydride species remained essentially unchanged and the formation of a Hf-propyl species could not be detected. On the other hand, more bulky olefins, which polymerize only slowly, led to the complete disappearance of the Hf-hydride signals. For example, whereas 3 equiv of 2,4,4-trimethyl-1-pentene added to a toluene-*d*₈/1,2-difluorobenzene solution of **9** (ca. 0.1 M) did not react at –10 °C, warming to room temperature led to the nearly complete disappearance of the peaks of **9**, accompanied by a corresponding drop in the trimethylpentene concentration. The signals of **9** were replaced by those of a new C_1 -symmetric hafnocene species (revealed by nonequivalent SiMe₂ peaks in the ^{13}C NMR spectrum); however, once again signals assignable to the Hf-CH₂- fragment could not be identified, and it remains uncertain whether the observed intermediate is a product of a single-insertion reaction.

In the second experiment, ca. 3 equiv of allylbenzene was added to a 0.1 M toluene-*d*₈/1,2-difluorobenzene solution of **9** at –10 °C. After warming the sample to room temperature, **9** was found to have been consumed completely, and at least two C_1 -symmetric hafnocene species were observed in the mixture. A ^{13}C NMR peak at $\delta 71.0$ (at –10 °C) was detected, indicating possibly the formation of a Hf-CH₂ species.

Activation of $\text{Me}_2\text{C}(\text{Cp})(\text{Flu})\text{HfCl}_2$ and $\text{Ph}_2\text{C}(\text{Cp})(\text{Flu})\text{HfCl}_2$ with $\text{AlBu}^i_3/\text{CPh}_3[\text{B}(\text{C}_6\text{F}_5)_4]$. Compounds **2** and **3** react with $\text{AlBu}^i_3/\text{CPh}_3[\text{B}(\text{C}_6\text{F}_5)_4]$ in a more complex way than **1**. The reaction products of **2** with this activator system gave a mixture of species that were too unstable at 2–5 °C to be identified. By contrast, the reaction of **3** with $\text{AlBu}^i_3/\text{CPh}_3[\text{B}(\text{C}_6\text{F}_5)_4]$ depends on the mixing temperature. Stirring the mixture (Hf:Al:B = 1:50:1.1) at 0 °C for 10 min resulted in a new C_s -symmetric ion pair as the predominant species, which, with its simple NMR spectrum, is most likely the chloro-bridged salt $[\{\text{Ph}_2\text{C}(\text{C}_5\text{H}_4)(\text{Flu})\text{Hf}(\mu\text{-Cl})_2\}]^{2+}[\text{B}(\text{C}_6\text{F}_5)_4]^{2-}$.²⁶ By contrast, mixing the

(22) (a) Bryliakov, K. P.; Babushkin, D. E.; Talsi, E. P.; Voskoboinikov, A. Z.; Gritzko, H.; Schröder, L.; Damrau, H.-R.; Wieser, U.; Schaper, F.; Brintzinger, H. H. *Organometallics* **2005**, *24*, 894. (b) Talsi, E. P.; Bryliakov, K. P.; Semikolenova, N. V.; Zakharov, V. A.; Bochmann, M. *Kinet. Catal.* **2007**, *48*, 490.

(23) Nedorezova, P. M.; Veksler, E. N.; Aladyshv, A. M.; Tsvetkova, V. I.; Optov, V. A.; Brusova, G. P.; Lemenovskii, D. A. *Kinet. Catal.* **2006**, *47*, 245.

(24) Nedorezova, P. M.; Veksler, E. N.; Optov, V. A.; Tsvetkova, V. I.; Sklyaruk, B. F. *Polym. Sci. Ser. A* **2007**, *49*, 99.

(25) Babushkin, D.; Panchenko, V. N.; Timofeeva, M. N.; Zakharov, V. A.; Brintzinger, H. H. *Macromol. Chem. Phys.* **2008**, *209*, 1210.

(26) For related chloro-bridged zirconocenes $[\{\text{Cp}^R_2\text{Zr}(\mu\text{-Cl})_2\}]^{2+}$ see ref 13 and: Wu, F.; Dash, A. K.; Jordan, R. F. *J. Am. Chem. Soc.* **2004**, *126*, 15360.

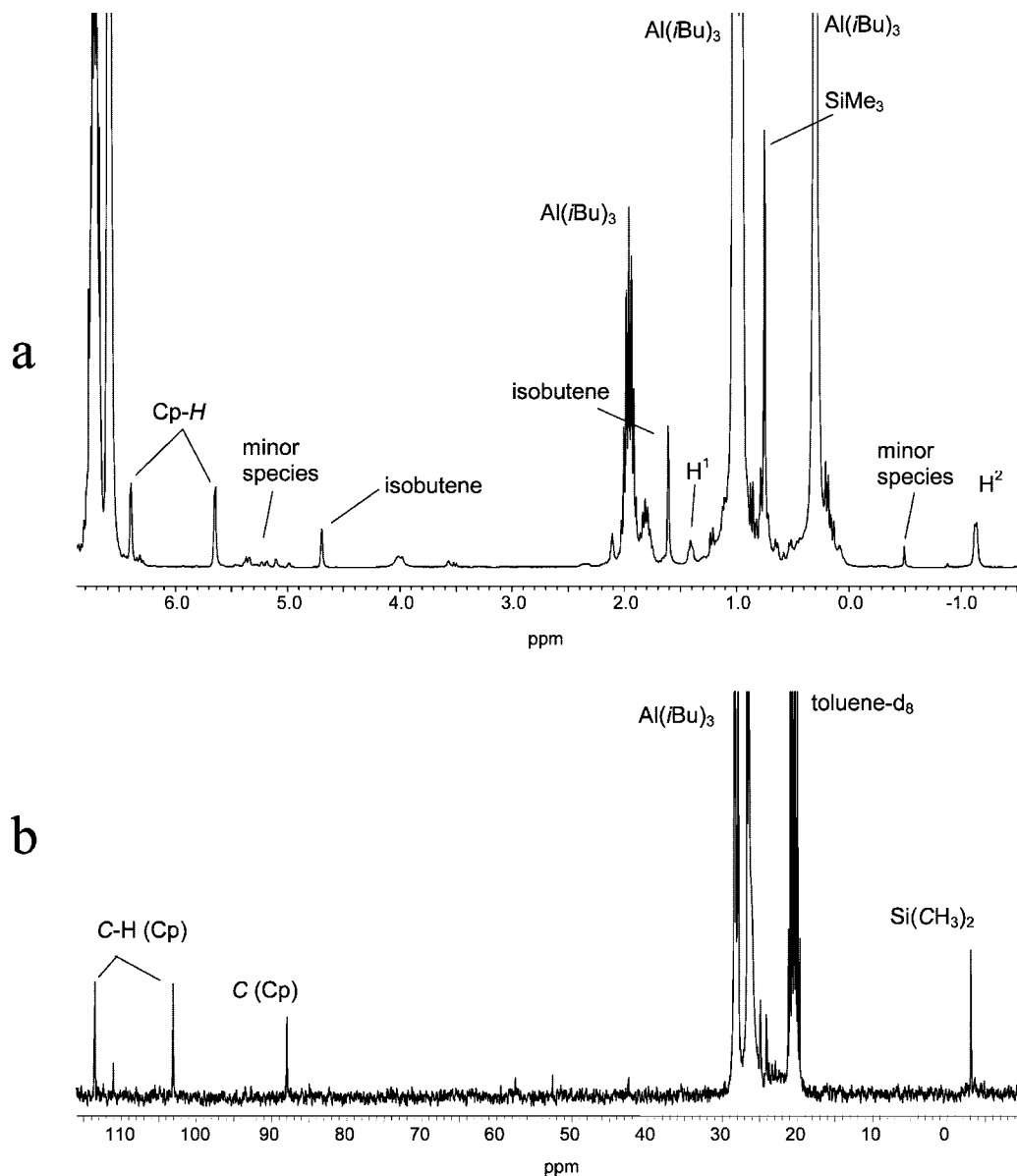
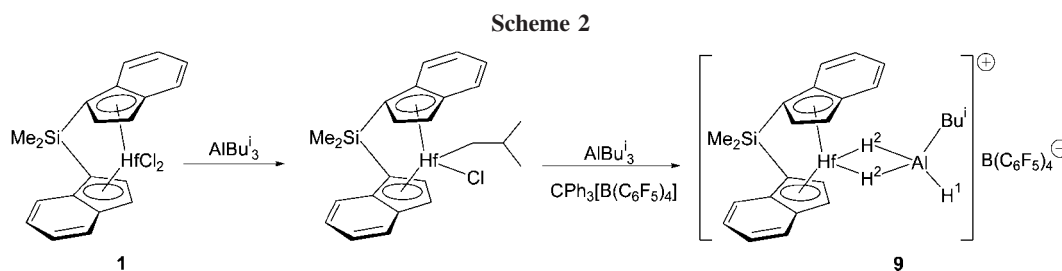


Figure 1. (a) ^1H and (b) ^{13}C NMR spectra of **9** obtained by the reaction of $(\text{SBI})\text{HfCl}_2$ (**1**) with $\text{AlBu}_3^i/\text{CPh}_3[\text{B}(\text{C}_6\text{F}_5)_4]$ ($\text{Hf}:\text{Al}:\text{B} = 1:50:1.1$; toluene- d_8 /1,2-difluorobenzene, 20°C).



reagents at 20°C for 1.5 h ($\text{Hf}:\text{Al}:\text{B} = 1:25\text{--}50:1.1$) gave rise to a new hafnium hydride species, **10**. One of the hydrides displays a ^1H NMR peak at $\delta -5.56$ (at $+2^\circ\text{C}$; 2H, dd, $J_{\text{HH}} = 13$ and 3.5 Hz). ^1H COSY spectra reveal that this signal shows a weak correlation with another signal at ca. $\delta 2.0$, which overlaps with intense peaks of toluene- d_8 and AlBu_3^i . This species was found to be an ion pair with the $[\text{B}(\text{C}_6\text{F}_5)_4]^-$ counteranion. The position of the ^1H hydride peak is charac-

teristic of bridging rather than terminal metallocene hydrides,^{13,14,27–31} however, the full structure could not be elucidated.

Reactions of $\text{C}_2\text{H}_4(\text{Flu})(5,6\text{-C}_3\text{H}_6\text{-2-MeInd})\text{HfCl}_2$ (4**).** As indicated in the Introduction, the hafnocene **4** is of interest since it produces high molecular weight elastomeric polypropylene

(28) Visser, C.; van den Hende, J. R.; Meetsma, A.; Hessen, B.; Teuben, J. H. *Organometallics* **2001**, *20*, 1620.

(29) Chirik, P. J.; Bercaw, J. E. *Organometallics* **2005**, *24*, 5407.

(30) Chung, J. H.; Lee, S. M. *Bull. Korean Chem. Soc.* **2006**, *27*, 759.

(31) Garratt, S.; Carr, A. G.; Langstein, G.; Bochmann, M. *Organometallics* **2003**, *36*, 4276.

(27) Grossman, R. B.; Doyle, R. A.; Buchwald, S. L. *Organometallics* **1991**, *10*, 1501.

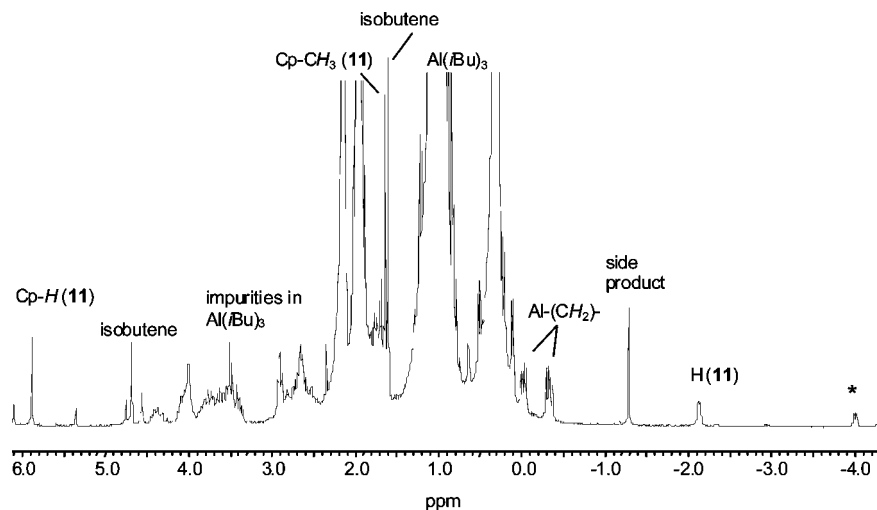


Figure 2. ^1H NMR spectrum (toluene- d_8 /1,2-difluorobenzene, 20 °C) of **11** obtained by the reaction of **4** with $\text{AlBu}_3^i/\text{CPh}_3[\text{B}(\text{C}_6\text{F}_5)_4]$ (Hf:Al:B = 1:100:1.1). The asterisk marks the hydride peak of the minor hafnium hydrido species.

and possesses two inequivalent sites for the σ -ligands. This complex was therefore studied in more detail.

Mixing **4** with $\text{AlBu}_3^i/\text{CPh}_3[\text{B}(\text{C}_6\text{F}_5)_4]$ (Hf:Al:B = 1:40–100:1) in toluene generates two types of hafnium hydride complexes that settle as a violet oil to the bottom of the NMR tube. As before, the upper phase was removed and the oil was dissolved in toluene- d_8 containing ca. 15 vol-% 1,2-difluorobenzene. Using a higher excess of AlBu_3^i along with longer reaction times leads to the formation of predominantly one hydride species, **11**, identified as $[\text{L}'\text{Hf}(\mu\text{-H})_2\text{AlBu}_2^i]^+[\text{B}(\text{C}_6\text{F}_5)_4]^-$. A typical ^1H NMR spectrum is shown in Figure 2.

The ^1H NMR spectrum of **11** shows a hydride resonance at δ -2.11 (1H, d, H^1 , $J_{\text{HH}} = 6$ Hz), which correlates with a second peak at δ 1.65. Apparently, due to the C_1 symmetry, two nonequivalent bridging hydrides are found at two very different chemical shifts. The Al-CH₂ peaks at δ -0.02 (2H, dd, $J_{\text{HH}} = 14$ and 7.2 Hz) and -0.33 (2H, dd, $J_{\text{HH}} = 14$ and 7.8 Hz) correlate with a signal at δ ca. 1.6, which apparently belongs to $\text{AlCH}_2\text{CHMe}_2$ groups. The peaks listed above appear and degrade in parallel with the Ind-*H* peak at δ 5.88 and Ind-*CH*₃ peak at δ 1.64; thus they can be ascribed to one and the same species **11**, the anionic part of which displays ^{19}F NMR signals at δ -132.5, -163.0, and -166.5. Ion pair **11** is unstable at room temperature and slowly decomposes (within 36 h). Warming the sample to 60 °C resulted in the loss of the hafnium hydride resonances. Species **11** reacts with 3 equiv of propene on warming from -20 to +10 °C.

Like **9**, species **11** reacts with 2,4,4-trimethyl-1-pentene: after the addition of 10 equiv of the alkene to the solution of **11** in toluene- d_8 /1,2-difluorobenzene ($[\text{11}] = 0.05$ M), the ^1H NMR signals of **11** had disappeared after 1 h at room temperature, while the minor hydride species (marked with an asterisk in Figure 2) remained unchanged.

In order to evaluate the ligand dynamics of C_1 -symmetric systems and evaluate the energy difference between the two possible alkyl ligand binding sites, we proceeded to prepare the mixed-alkyl complex $\text{C}_2\text{H}_4(\text{Flu})(5,6\text{-C}_3\text{H}_6\text{-2-MeInd})\text{-Hf}(\text{Me})\text{CH}_2\text{SiMe}_3$ and the corresponding $[\text{L}'\text{Hf-CH}_2\text{SiMe}_3]^+$ cation.

There was no significant reaction between the dichloride complex **4** and $\text{Me}_3\text{SiCH}_2\text{MgCl}$ until the mixture was heated to 80 °C. The preferred solvent for this reaction is toluene. Under these conditions, the reaction is selective for the monoalkylation product $\text{L}'\text{Hf}(\text{Cl})\text{CH}_2\text{SiMe}_3$ (**12**). One of the two possible

isomers strongly predominates. There is evidence for the presence of a minor second isomer in the crude reaction mixture, but only the major isomer could be crystallized. The solid state structure is shown in Figure 3.

The metallocene geometry resembles that of (SBI)Hf-(Me)(CH₂SiMe₃).¹⁶ The bond lengths to the trimethylsilylmethyl ligands and the angles to the second ligands in both complexes are experimentally indistinguishable. The difference in bonding to the fluorenyl and indenyl parts of the ligand is reflected in the Hf-C_{Ind} and Hf-C_{Flu} distances of 2.22 and 2.30 Å, respectively. The fluorenyl also exhibits greater variation in the Hf-C bond lengths, between 2.428(8) and 2.605(8) Å, but they are all sufficiently short to designate η^5 hapticity.

The most striking feature of the molecular structure of **12** is that this major product is not the one predicted based on steric considerations: the trimethylsilylmethyl ligand is bound on the apparently more hindered side of the metallocene wedge, adopting a conformation whereby the alkyl ligand is located in close proximity to both the fluorenyl and indenyl six-membered rings. This isomer is produced with high stereoselectivity, presumably under kinetic control. A possible explanation is that in the precursor **4** the same steric interactions slightly weaken the Hf-Cl bond in that position, such that substitution of that chlorine atom is kinetically favored.³² This finding urges caution when predicting reaction outcomes based on *prima facie* steric considerations.

The mixed-alkyl complex $\text{L}'\text{Hf}(\text{Me})\text{CH}_2\text{SiMe}_3$ (**13**) was prepared in a two-step, two-pot procedure from **4**, but without isolating the intermediate **12**. Complex **13** is very poorly soluble in light petroleum, but highly soluble in toluene. Attempts to crystallize **13** from toluene/light petroleum mixtures led only to the precipitation of a fine solid, which trapped impurities. A sample pure enough for subsequent spectroscopic studies was isolated by extracting the crude product with toluene/light petroleum, followed by removal of the solvents and washing the residue with light petroleum.

Surprisingly, while the diastereotopic Hf-CH₂ group of the chloro trimethylsilylmethyl complex gives the expected pair of doublets in the chloroform- d_1 ^1H NMR spectrum, the Hf-CH₂ signal of the methyl trimethylsilylmethyl appears as a singlet.

(32) Evidence that the coordination site occupied by Cl in **12** is the less hindered one is also provided by the equilibrium between cations **14a** and **14b**, where **14a** is the dominant species.

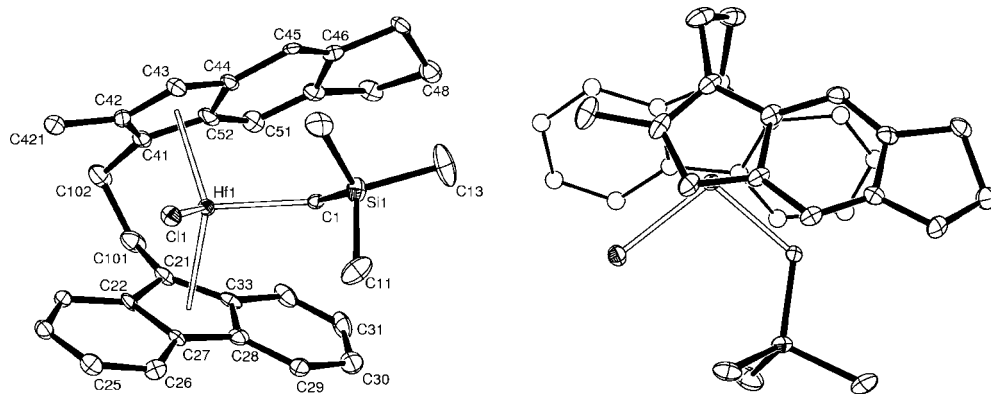
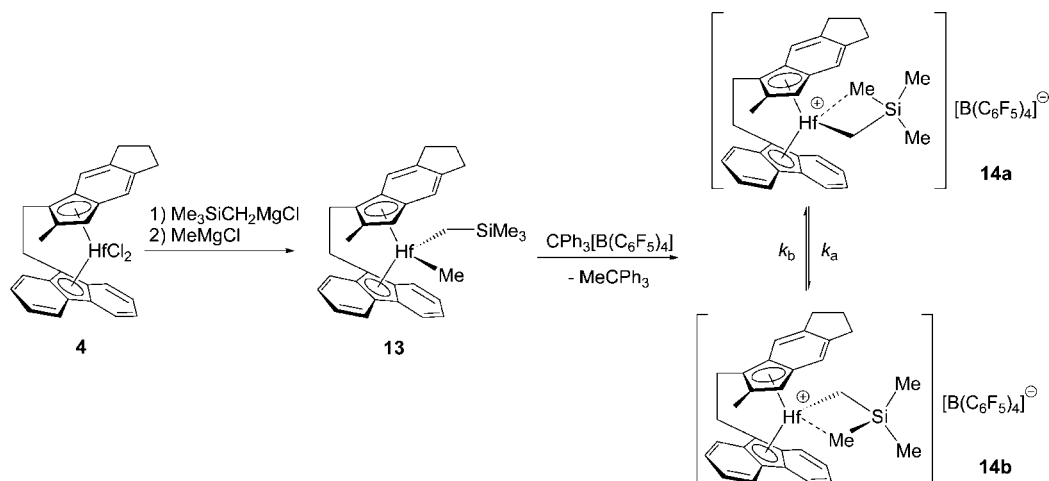


Figure 3. Left: Molecular structure of $L'Hf(Cl)CH_2SiMe_3$ (**12**), showing the atomic numbering scheme. Displacement ellipsoids are drawn at the 30% probability level. Hydrogen atoms have been omitted for clarity. Selected bond length (\AA) and angles (deg, esd's are in parentheses): Hf(1)–C(1) 2.224(8); Hf(1)–Cl(1), 2.4143(19), Hf(1)–C(21) 2.428(8), Hf(1)–C(41) 2.473(8), Hf(1)–C(42) 2.488(9), Hf(1)–C(43) 2.511(9), Hf(1)–C(22) 2.547(7), Hf(1)–C(52) 2.547(8), Hf(1)–C(33) 2.605(8), Hf(1)–C(44) 2.623(8), Hf(1)–C(27) 2.699(7), Hf(1)–C(28) 2.737(8), Hf(1)–Ct_{Flu} 2.304, Hf(1)–Ct_{Ind} 2.22; C(1)–Hf(1)–Cl(1) 101.27(19), Ct_{Ind}–Hf(1)–Ct_{Flu} 128.4, Si(1)–C(1)–Hf(1) 122.6(4) (Ct_{Flu} = centroid of the fluorenyl ring; Ct_{Ind} = centroid of the indenyl ring). Right: View of **12** perpendicular to the Cl–Hf–C(1) plane, illustrating the steric environment of the CH_2SiMe_3 ligand.

Scheme 3



The identity of the resonance was confirmed by HETCOR and DEPT experiments. It therefore appears that in chloroform- d_1 both Hf- CH_2 hydrogen atoms have coincidentally identical chemical shifts. In toluene- d_8 the diastereotopic Hf- CH_2 protons appear separately in the 1H NMR spectra at temperatures up to +40 $^\circ C$.

Treatment of **13** with $CPh_3[B(C_6F_5)_4]$ in toluene affords $[L'HfCH_2SiMe_3]^+[B(C_6F_5)_4]^-$ (**14**) as a red-brown oil (Scheme 3).³³ At low temperatures (-40 to 0 $^\circ C$), the ^{13}C and 1H NMR spectra show two diastereomers, **14a** and **14b**, which differ in the site of CH_2SiMe_3 coordination (Figure 4). At -20 $^\circ C$, the ratio of major and minor isomers was found to be 1.6:1. In both structures, three separate 1H NMR signals were found for the $SiMe_3$ groups, with the high-field resonances (at δ -1.58 for the minor isomer and δ -2.58 for the major one) indicating the γ -agostic bonding of one of the CH_3 groups.^{15–17} The position of the CH_2SiMe_3 ligand in **14a** and **14b** was determined from the $^1H, ^1H$ NOESY spectrum: in the major isomer, a NOE correlation peak (at 300 ms mixing time) between one of the

Hf- CHH -Si and the Cp- CH_3 protons was observed, thus leading to a conclusion that the structure of the major isomer corresponds to that of **14a** (Scheme 3 and Supporting Information). The most thermodynamically stable cation therefore appears to be that where the trimethylsilylmethyl ligand is located in the alternative position to the chloro trimethylsilylmethyl complex **12**.

The interconversion of **14a** and **14b** leads to a broadening of the spectra with increasing temperature; coalescence is reached at +25 $^\circ C$. Given the low ligand symmetry, the site epimerization is characterized by two different exchange rate constants (such that $k_a[14a] = k_b[14b]$), and the characteristic time of the overall exchange process $\tau_{ex} = (k_a + k_b)^{-1}$. This leads to estimates for $k_a = 1.1 \times 10^2$ s^{-1} and $k_b = 1.8 \times 10^2$ s^{-1} and for ΔG_a^\ddagger and ΔG_b^\ddagger (at the coalescence temperature of 298 K) = 14.7 and 14.4 kcal mol^{-1} , respectively.³⁴ These values are close to that observed for the $[(SBI)Hf(CH_2SiMe_3)]^+[B(C_6F_5)_4]^-$ ion pair.¹⁶

(33) For the related activation of mixed-alkyl Zr and Hf complexes with $B(C_6F_5)_3$ see: Beswick, C. L.; Marks, T. J. *J. Am. Chem. Soc.* **2000**, *122*, 10358. For the reaction of $[(SBI)ZrCH_2SiMe_3][B(C_6F_5)_4]$ with 1-hexene see: Landis, C. R.; Christianson, M. D. *Proc. Natl. Acad. Sci.* **2006**, *103*, 15349.

(34) To estimate the exchange rate constants, the Cp- H 1H NMR peaks were considered, assuming the $\Delta\omega_0 = 290$ Hz (at -40 $^\circ C$) and coalescence temperature +25 $^\circ C$. At temperatures lower than -40 $^\circ C$, the 1H NMR peaks of **7a** and **7b** become too broad due to the increased viscosity of the toluene/difluorobenzene solvent.

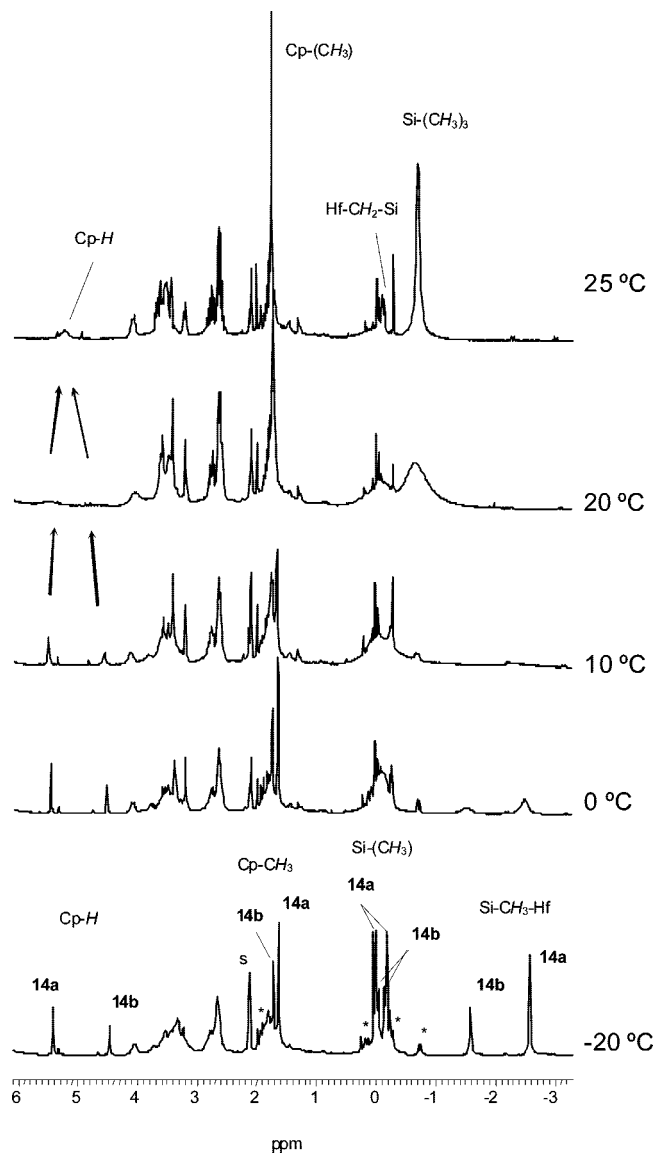


Figure 4. ^1H NMR spectrum (toluene- d_8 /1,2-difluorobenzene) of the cationic hafnium species obtained by the reaction of **14** with $\text{CPh}_3[\text{B}(\text{C}_6\text{F}_5)_4]$ ($\text{Hf}:\text{B} = 1:1.1$) at differing temperatures. Asterisks mark the $\text{Hf}-\text{CHH}-\text{Si}$ peaks of both major (**14a**) and minor (**14b**) isomers.

Of particular interest is the question of the relation between the chain propagation rate and the observed site epimerization rate. For the system **4**/ $\text{AlBu}_3/\text{CPh}_3[\text{B}(\text{C}_6\text{F}_5)_4]$, Rieger and co-workers reported an increase in isotacticity of propene polymerization with temperature ([mmmm] fraction rising from 17 to 34% upon increasing the polymerization temperature from 0 to 50 °C) and explained this by a favored back-skip of the growing polymer chain before monomer coordination.^{1–3} One should expect then that the back-skip and chain propagation processes should have comparable rates. The observed site epimerization in **14** can be regarded as a model of this back-skip process, providing the kinetic parameters of this exchange. From the reported polymerization data of Rieger under pseudo-

first-order conditions one can derive the propagation rate constants k_p^{obs} (estimated from the polymer yield) of 150 s^{-1} at 20 °C and 330 s^{-1} at 50 °C. These values are very comparable to the site epimerization rates observed here for **14** and thus support the conclusion that the back-skip and chain propagation processes proceed with comparable rates.^{35,36}

Conclusions

The interaction of hafnocenes **1–3** with MAO, $\text{AlMe}_3/\text{CPh}_3[\text{B}(\text{C}_6\text{F}_5)_4]$, and $\text{AlBu}_3/\text{CPh}_3[\text{B}(\text{C}_6\text{F}_5)_4]$ lead to different types of cationic intermediates with different reactivities. The methyl-bridged heterobinuclear intermediates $[\text{LHf}(\mu\text{-Me})_2\text{Al}(\mu\text{-Me})_2][\text{MeMAO}]$ and $[\text{LHf}(\mu\text{-Me})_2\text{Al}(\mu\text{-Me})_2][\text{B}(\text{C}_6\text{F}_5)_4]$ are thermally stable at room temperature but display only low olefin polymerization productivities; that is, they polymerize propene only on warming to room temperature. The stability of these $\mu\text{-Me}$ products is thought to be responsible for the comparatively low catalytic activity of hafnocenes when AlMe_3 is present (i.e., with AlMe_3 -rich MAO). Activation with $\text{AlBu}_3/\text{CPh}_3[\text{B}(\text{C}_6\text{F}_5)_4]$, on the other hand, generates heterobinuclear hydrido-bridged species of the type $[\text{LHf}(\mu\text{-H})_2\text{AlBu}_2]^+$ or $[\text{LHf}(\mu\text{-H})_2\text{Al}(\text{H})\text{Bu}]^+$, which are much more reactive in olefin polymerizations. The hafnium hydride species were completely consumed in reactions with a few equivalents of 2,4,4-trimethyl-1-pentene and allylbenzene, thus confirming their role as the active site precursors.

Similar reactions were found for the C_1 -symmetric hafnocene **4**. The two chloride ligands show surprisingly different reactivity, as shown by the stereoselective synthesis of $\text{L}^*\text{Hf}(\text{Cl})\text{CH}_2\text{SiMe}_3$. The ion pair $[\text{C}_2\text{H}_4(\text{Flu})(5,6\text{-C}_3\text{H}_6\text{-2-MeInd})\text{HfCH}_2\text{SiMe}_3]^+[\text{B}(\text{C}_6\text{F}_5)_4]^-$ produced on trityl borate activation exists as a mixture of two diastereomers, which are in equilibrium. The site epimerization rates indicate that the two possible alkyl ligand coordination sites are of very comparable energy; these rates are also of the same order of magnitude as propagation rates for propene polymerizations with this system.

Experimental Section

Methylaluminoxane (MAO) was purchased from Crompton GmbH (Germany) as a toluene solution (total Al content 1.8 M, Al as AlMe_3 0.5 M). Ethylene- $^{13}\text{C}_2$ (99% ^{13}C) was purchased from Aldrich. Triisobutylaluminum (AlBu_3) was purchased from Aldrich and either diluted to obtain a solution of $[\text{Al}] = 1 \text{ M}$ or used as received for experiments with high Al/Hf ratios. Trimethylaluminum (AlMe_3) was purchased from Aldrich as a 2 M solution in toluene. Toluene was purified by refluxing over sodium metal and distilled under dry nitrogen. 1,2-Difluorobenzene was dried over molecular sieves (4 Å) and degassed. All operations were carried out under dry nitrogen (99.999%) by standard Schlenk techniques. Solids and toluene were transferred and stored in a glovebox. $(\text{SBI})\text{HfCl}_2$ (**1**),³⁷ $\text{Me}_2\text{C}(\text{Cp})(\text{Flu})\text{HfCl}_2$ (**2**),³⁸ $\text{Ph}_2\text{C}(\text{Cp})(\text{Flu})\text{HfCl}_2$ (**3**),³⁹ and $\text{CPh}_3[\text{B}(\text{C}_6\text{F}_5)_4]$ ⁴⁰ were prepared according to literature procedures. Complex $\text{C}_2\text{H}_4(\text{Flu})(5,6\text{-C}_3\text{H}_6\text{-2-MeInd})\text{HfCl}_2$ (**4**) was kindly donated by Prof. B. Rieger.

^1H , $^{13}\text{C}\{^1\text{H}\}$, and ^{19}F NMR spectra were recorded in standard 5 mm NMR tubes on either Bruker Avance DPX-300 or Avance 400 spectrometers. Typical operating conditions for ^{13}C NMR measure-

(35) One should be aware, however, that k_p^{obs} estimated from the polymer yield might be ca. 1 order of magnitude lower than that determined from the time dependence of the number-average molecular weight at the initial stages of polymerization.^{15,36}

(36) (a) Song, F.; Cannon, R. D.; Bochmann, M. *J. Am. Chem. Soc.* **2003**, *125*, 7641. (b) Song, F.; Cannon, R. D.; Lancaster, S. J.; Bochmann, M. *J. Mol. Catal.* **2004**, *218*, 21.

(37) Herrmann, W. A.; Rohmann, J.; Herdtweck, E.; Spaleck, W.; Winter, A. *Angew. Chem., Int. Ed. Engl.* **1989**, *28*, 1511.

(38) Ewen, J. A.; Jones, R. L.; Razavi, A.; Ferrara, J. D. *J. Am. Chem. Soc.* **1988**, *110*, 6255.

(39) Mise, T.; Miya, S.; Yamazaki, H. *Chem. Lett.* **1989**, 1853.

(40) Bochmann, M.; Lancaster, S. J. *J. Organomet. Chem.* **1992**, *434*, C1.

ments were the following: spectral width 20 kHz; spectrum accumulation frequency 0.1 Hz; 100–5000 transients, 90° pulse at 6.7 μ s. Correct integral values were obtained from inverse gated spectra. ^{13}C , ^1H correlations were established by using the standard Bruker HXCOBI (for direct C–H interactions) pulse program. Operating conditions for ^1H NMR measurements: spectral width 5 kHz; spectrum accumulation frequency 0.2–0.5 Hz; number of transients 32–64, ca. 30° pulse at 2 μ s. Typical operating conditions for ^{19}F NMR measurements: spectral width 30 kHz; spectrum accumulation frequency 0.1–0.5 Hz; number of transients 32–64. For calculations of ^1H and ^{13}C chemical shifts, the resonance of the CH_3 group of toluene solvent was taken as δ 2.09 and 20.40, respectively. ^{19}F chemical shifts were referenced externally to CFCl_3 . Sample temperature measurement uncertainty and temperature reproducibility were less than ± 1 °C.

Preparation of MAO and Al_2Me_6 Samples. Solid MAO was prepared from commercial MAO (Crompton) by removal of the solvent under vacuum at 20 °C. The solid product obtained (polymeric MAO with total Al content 40 wt % and Al as residual AlMe_3 ca. 5 wt %) was used for the preparation of the samples. ^{13}C -enriched MAO was prepared by ligand exchange of 99% ^{13}C -enriched Al_2Me_6 (70 mol % of total Me groups) and solid MAO (30 mol % of total Me groups) in toluene solution followed by subsequent removal of the liquid fraction of Al_2Me_6 under vacuum to give a sample of ^{13}C -enriched MAO (65–70% ^{13}C) with desired Al_2Me_6 content (polymeric MAO with total Al content of 40% and Al as residual AlMe_3 ca. 5 wt %). A more detailed description is presented in ref 41.

Preparation of NMR Samples. The appropriate amounts of hafnium complex (typically, 0.01–0.06 mmol) and MAO or $\text{CPh}_3[\text{B}(\text{C}_6\text{F}_5)_4]$ were placed in 5 mm NMR tubes in a glovebox and capped with rubber septa. Further addition of AlMe_3 solution (if necessary, Al/Hf = 30–50) to the tube with the hafnium complex was performed outside the glovebox with gastight microsyringes. For hafnocenes/MAO samples, the spectra were recorded in toluene.

For hafnocenes/ $\text{AlMe}_3/\text{CPh}_3[\text{B}(\text{C}_6\text{F}_5)_4]$ systems, the resulting cationic species were poorly soluble in toluene but formed oily precipitates in the lower part of the NMR tube. Normally, after shaking the samples at room temperature, they were allowed to stand to achieve the phase separation, then the upper (toluene) phase was removed and the oily residue was dissolved in 0.5 mL of toluene- d_8 and 0.1 mL of 1,2-difluorobenzene to obtain a homogeneous solution.

For hafnocenes/ $\text{AlBu}_3/\text{CPh}_3[\text{B}(\text{C}_6\text{F}_5)_4]$ systems, in a glovebox the appropriate amounts of hafnium complex (typically, 0.03–0.06 mmol) and $\text{CPh}_3[\text{B}(\text{C}_6\text{F}_5)_4]$ were placed in a Schlenk tube equipped with a magnetic stirrer and capped with a rubber septum. Further addition of AlBu_3 solution was performed outside the glovebox with gastight microsyringes at 0 °C, and the mixture was then stirred at room temperature (typically 1–2 h). The oily phase was allowed to settle and the upper toluene phase was decanted. This removed most (but not all) of the excess AlBu_3 . The oil was dissolved in toluene- d_8 and 1,2-difluorobenzene (5:1 v/v), and the resulting samples were taken for the NMR measurements.

Propene and ethene (^{13}C -ethene) were injected in the NMR tubes via gastight syringes upon appropriate cooling (below –30 °C).

Typical NMR Data for the $[\text{B}(\text{C}_6\text{F}_5)_4]^-$ Counteranion. $^{13}\text{C}\{^1\text{H}\}$ NMR (75.47 MHz, toluene- d_8 , 1,2-difluorobenzene, 20 °C): δ 148.9 (8C, *o*-C, $J_{\text{CF}}^1 = 246$ Hz), 138.7 (d, 4C, *p*-C, $J_{\text{CF}}^1 = 246$ Hz), 136.9 (d, 8C, *m*-C, $J_{\text{CF}}^1 = 245$ Hz). ^{19}F NMR (282.40 MHz, toluene- d_8 , 1,2-difluorobenzene, 20 °C): δ –132.5 (2F, *o*-F), –163.0 (t, 1F, *p*-F, $J_{\text{FF}}^3 = 19$ Hz), –166.5 (2F, *m*-F).

(SBI)HfMeCl. ^1H NMR (300.13 MHz, toluene- d_8 /1,2-difluorobenzene, 20 °C, $\text{Al}_{\text{MAO}}/\text{Hf} = 30$): δ 6.62 (d, 1H, Cp-*H*, $J_{\text{HH}} =$

3.0 Hz), 6.49 (d, 1H, Cp-*H*, $^3J_{\text{HH}} = 3.0$ Hz), 5.94 (d, 1H, Cp-*H*, $J_{\text{HH}} = 3.0$ Hz), 5.42 (d, 1H, Cp-*H*, $J_{\text{HH}} = 3.0$ Hz), 0.64 (s, 3H, SiMe), 0.54 (s, 3H, SiMe), –0.82 (s, 3H, HfMe). $^{13}\text{C}\{^1\text{H}\}$ NMR (75.47 MHz, toluene- d_8 /1,2-difluorobenzene, 20 °C, Al/Hf = 30, ^{13}C -enriched MAO used): δ 41.2 (1C, Hf-Me, $J_{\text{CH}}^1 = 124$ Hz).

[(SBI)Hf(μ -Me) $_2$ AlMe $_2$][MeMAO] (5-MAO). ^1H NMR (300.13 MHz, toluene- d_8 /1,2-difluorobenzene, 20 °C, Al/Hf = 240): δ 6.17 (2H, Cp-*H*), 5.05 (2H, Cp-*H*), 0.80 (s, 6H, SiMe $_2$), –0.60 (s, 6H, AlMe $_2$), –0.90 (s, 3H, Hf(μ -Me) $_2$ Al). $^{13}\text{C}\{^1\text{H}\}$ NMR (75.47 MHz, toluene- d_8 /1,2-difluorobenzene, 20 °C, Al/Hf = 240, ^{13}C -enriched MAO used): δ 35.7 (2C, Hf(μ -Me) $_2$ Al, $J_{\text{CH}}^1 = 113$ Hz).

[(SBI)Hf(μ -Me) $_2$ AlMe $_2$][B(C $_6$ F $_5$) $_4$] (5-BX $_4$). ^1H NMR (300.13 MHz, toluene- d_8 /1,2-difluorobenzene, 20 °C): δ 6.10 (d, 2H, Cp-*H*, $J_{\text{HH}} = 3.2$ Hz), 5.00 (d, 2H, Cp-*H*, $J_{\text{HH}} = 3.2$ Hz), 0.75 (s, 6H, SiMe $_2$), –0.70 (s, 6H, AlMe $_2$), –0.93 (s, 6H, Hf(μ -Me) $_2$ Al); 2.00 (s, 3H, Ph $_3$ CCH $_3$). ^{13}C NMR (75.47 MHz, toluene- d_8 /1,2-difluorobenzene, 20 °C): δ 115.8 (2C, Cp, $J_{\text{CH}}^1 = 179$ Hz), 113.9 (2C, Cp, $J_{\text{CH}}^1 = 179$ Hz), 86.4 (2C, Si-C(Cp)), 35.2 (2C, Hf(μ -Me) $_2$ Al, $J_{\text{CH}}^1 = 113$ Hz), –3.2 (2C, SiMe $_2$, $J_{\text{CH}}^1 = 122$ Hz), –7.2 (2C, AlMe $_2$, $J_{\text{CH}}^1 = 115$ Hz).

Me $_2$ C(Cp)(Flu)HfMeCl. ^1H NMR (400.13 MHz, toluene- d_8 /1,2-difluorobenzene, 20 °C, Al/Hf = 90): δ 6.10 (1H, Cp-*H*), 5.75 (1H, Cp-*H*), 5.45 (1H, Cp-*H*), 4.95 (1H, Cp-*H*), 1.85 (s, 3H, CMe), 1.77 (s, 3H, CMe), –1.06 (s, 3H, HfMe).

[Me $_2$ C(Cp)(Flu)Hf(μ -Me) $_2$ AlMe $_2$][MeMAO] (6-MAO). ^1H NMR (400.13 MHz, toluene- d_8 , 20 °C, Al/Hf = 300): δ 5.68 (2H, Cp-*H*), 4.76 (2H, Cp-*H*), 1.98 (s, 6H, C(CH $_3$) $_2$). AlMe $_2$ and Hf(μ -Me) $_2$ Al peaks not observed (hidden by broad and intense MAO signal).

[Me $_2$ C(Cp)(Flu)Hf(μ -Me) $_2$ AlMe $_2$][B(C $_6$ F $_5$) $_4$] (6-BX $_4$). ^1H NMR (400.13 MHz, toluene- d_8 /1,2-difluorobenzene, 20 °C): δ 5.63 (2H, Cp-*H*), 4.74 (2H, Cp-*H*), 1.90 (s, 6H, CMe $_2$), –0.72 (s, 3H, AlMe), –0.81 (s, 3H, AlMe), –1.11 (s, 6H, Hf(μ -Me) $_2$ Al). ^{13}C NMR (100.614 MHz, toluene- d_8 /1,2-difluorobenzene, 20 °C): δ 118.0 (2C, Cp), 102.2 (2C, Cp), 28.1 (2C, Hf(μ -Me) $_2$ Al), 27.7 (2C, CMe $_2$), –6.5 (2C, AlMe), –9.0 (2C, AlMe).

Ph $_2$ C(Cp)(Flu)HfMeCl. ^1H NMR (400.13 MHz, toluene- d_8 , 20 °C, $\text{Al}_{\text{MAO}}/\text{Hf} = 90$): δ 6.50 (1H, Cp-*H*), 6.30 (1H, Cp-*H*), 5.90 (1H, Cp-*H*), 5.45 (1H, Cp-*H*), –1.08 (s, 3H, HfMe).

[Ph $_2$ C(Cp)(Flu)Hf(μ -Me) $_2$ AlMe $_2$][MeMAO] (7-MAO). ^1H NMR (400.13 MHz, toluene- d_8 , 20 °C, Al/Hf = 300): δ 6.15 (2H, Cp-*H*), 5.15 (2H, Cp-*H*), –1.05 (6H, Hf(μ -Me) $_2$ Al).

[Ph $_2$ C(Cp)(Flu)Hf(μ -Me) $_2$ AlMe $_2$][B(C $_6$ F $_5$) $_4$] (7-BX $_4$). ^1H NMR (400.13 MHz, toluene- d_8 /1,2-difluorobenzene, 20 °C): δ 6.05 (2H, Cp-*H*), 5.12 (2H, Cp-*H*), –0.64 (s, 3H, Al(CH $_3$)), –0.79 (s, 3H, AlMe), –1.09 (s, 6H, Hf(μ -Me) $_2$ Al). ^{13}C NMR (100.614 MHz, toluene- d_8 /1,2-difluorobenzene, 20 °C): δ 123.1 (2C, Cp), 111.4 (2C, Cp), 99.0 (C, C(Cp)), 63.3 (1C, CPh $_2$), 30.6 (2C, Hf(μ -Me) $_2$ Al), –6.3 (2C, AlMe), –9.1 (2C, AlMe).

[C $_2$ H $_4$ (Flu)(5,6-C $_3$ H $_6$ -2-MeInd)Hf(μ -Me) $_2$ AlMe $_2$][MeMAO] (8-MAO). ^1H NMR (300.13 MHz, toluene- d_8 , 20 °C, Al/Hf = 90): δ 5.41 (s, 1H, Cp-*H*), 1.79 (s, 3H, Cp-CH $_3$), –0.6 (s, 3H), –0.75 (s, 3H, AlMe), –1.94 (s, 3H, Hf(μ -Me) $_2$ Al). ^{13}C NMR (75.47 MHz, toluene- d_8 /1,2-difluorobenzene, 20 °C, ^{13}C -enriched MAO was used): δ 103.5 (1C, Cp), 103.2 (1C, Cp-*H*, $J_{\text{CH}}^1 = 178$ Hz), 36.7 (1C, Hf(μ -Me) $_2$ Al, $J_{\text{CH}}^1 = 112$ Hz), 36.3 (1C, Hf(μ -Me) $_2$ Al, $J_{\text{CH}}^1 = 112$ Hz), 14.2 (1C, Cp-CH $_3$, $J_{\text{CH}}^1 = 130$ Hz), –6.1 (1C, AlMe, $J_{\text{CH}}^1 = 113$ Hz), –7.8 (1C, AlMe, $J_{\text{CH}}^1 = 113$ Hz).

[C $_2$ H $_4$ (Flu)(5,6-C $_3$ H $_6$ -2-MeInd)Hf(μ -Me) $_2$ AlMe $_2$] $^+[\text{B}(\text{C}_6\text{F}_5)_4]^-$ (8-BX $_4$). ^1H NMR (300.13 MHz, toluene- d_8 /1,2-difluorobenzene, 20 °C): δ 5.38 (s, 1H, Cp-*H*), 1.71 (s, 3H, Cp-CH $_3$), –0.69 (s, 3H, AlMe), –0.74 (s, 3H, Hf(μ -Me) $_2$ Al), –0.82 (s, 3H, AlMe), –1.88 (s, 3H, Hf(μ -Me) $_2$ Al); 2.00 (s, 3H, Ph $_3$ CCH $_3$). ^{13}C NMR (75.47 MHz, toluene- d_8 /1,2-difluorobenzene, 10 °C): δ 103.5 (1C, Cp), 103.2 (1C, Cp-*H*, $J_{\text{CH}}^1 = 178$ Hz), 36.2 (1C, Hf(μ -Me) $_2$ Al, $J_{\text{CH}}^1 = 112$ Hz), 36.1 (1C, Hf(μ -Me) $_2$ Al, $J_{\text{CH}}^1 = 112$ Hz), 14.2 (1C, Cp-

CH_3 , $J^1_{\text{CH}} = 130$ Hz), -6.1 (1C, AlMe), $J^1_{\text{CH}} = 113$ Hz), -7.8 (1C, AlMe, $J^1_{\text{CH}} = 113$ Hz).

(SBI)Hf(Bu¹)Cl. ^1H NMR (300.13 MHz, toluene- d_8 , 20 °C, Al/Hf = 90): δ 5.88 (d, 1H, Cp-H, $J_{\text{HH}} = 3.0$ Hz), 5.36 (s, 1H, Cp-H, $J_{\text{HH}} = 3.0$ Hz), 0.62 (s, 3H, SiMe), 0.51 (s, 3H, SiMe), -0.72 (dd, 1H, Hf-CH₂), $J_{\text{HH}} = 14$ Hz, $J_{\text{HH}} = 7$ Hz), -1.11 (dd, 1H, Hf-CH₂, $J_{\text{HH}} = 14$ Hz, $J_{\text{HH}} = 5$ Hz). Isobutene: δ 4.65 (s, 2H, CH₂), 1.59 (s, 6H, Me). ^{13}C NMR (75.47 MHz, toluene- d_8 , 1,2-difluorobenzene, 20 °C): δ 80.4 (1C, Hf-CH₂, $J^1_{\text{CH}} = 113$ Hz), -1.8 (1C, SiMe), -2.4 (1C, SiMe).

[(SBI)Hf(μ -H)₂Al(H)(Bu¹)⁺[B(C₆F₅)₄]⁻ (9). ^1H NMR (300.13 MHz, toluene- d_8 , 20 °C, Al/Hf = 90): δ 6.38 (d, 2H, Cp-H, $^2J_{\text{HH}} = 2.8$ Hz), 5.64 (s, 2H, Cp-H, $J_{\text{HH}} = 2.8$ Hz), 1.40 (t, 1H, hydride, $J_{\text{HH}} = 5$), 0.75 (s, 6H, SiMe), -1.13 (d, 2H, hydride, $J_{\text{HH}} = 5$ Hz). Isobutene: δ 4.69 (s, 2H, CH₂), 1.60 (s, 6H, Me). ^{13}C NMR (75.47 MHz, toluene- d_8 , 1,2-difluorobenzene, 20 °C): δ 113.4 (2C, C-H (Cp)), $J^1_{\text{CH}} = 172$ Hz), 103.1 (2C, C-H (Cp), $J^1_{\text{CH}} = 179$ Hz), 87.9 (2C, C (Cp)), -3.2 (2C, SiMe₂).

[[Ph₂C(C₅H₄)(Flu)Hf(μ -Cl)]₂]²⁺·2[B(C₆F₅)₄]⁻. ^1H NMR (400.13 MHz, toluene- d_8 /1,2-difluorobenzene, 20 °C): δ 6.16 (4H, Cp-H), 5.08 (4H, Cp-H). ^{13}C NMR (100.614 MHz, toluene- d_8 /1,2-difluorobenzene, 20 °C): δ 126.6 (4C, C-H, (Cp)), 112.0 (4C, C-H, (Cp)), 100.5 (2C, C(Cp)), 63.3 (2C, CPh₂).

Activation of Ph₂C(Cp)(Flu)HfCl₂ with AlBu¹₃/CPh₃[B(C₆F₅)₄](Hf:Al:B = 1:25–50:1.1): Species 10. ^1H NMR (400.13 MHz, toluene- d_8 /1,2-difluorobenzene, 20 °C): δ 6.22 (1H, Cp-H, $J_{\text{HH}} = 2$ Hz), 5.37 (1H, Cp-H, $J_{\text{HH}} = 2$ Hz), 5.08 (1H, Cp-H, $J_{\text{HH}} = 2$ Hz), 2.0, -5.56 (1H, $J_{\text{HH}} = 13$ Hz, $J_{\text{HH}} = 3.5$ Hz). ^{13}C NMR (100.614 MHz, toluene- d_8 /1,2-difluorobenzene, 20 °C): δ 123.0 (1C, quaternary C), 118.6 (1C, C–H, (Cp)), 113.6 (1C, C–H, (Cp)), 112.2 (1C, Cp), 97.6 (1C, C(Cp)), 59.9 (1C, CPh₂).

[C₂H₄(Flu)(5,6-C₃H₆-2-MeInd)Hf(μ -H)₂AlBu¹]⁺[B(C₆F₅)₄]⁻ (11). ^1H NMR (300.13 MHz, toluene- d_8 , 20 °C, Al/Hf = 90): δ 5.88 (s, 1H, Cp-H), 1.64 (s, 1H, Cp-CH₃), -0.02 (2H, dd, Al(CHH)₂, $J_{\text{HH}} = 14$ Hz, $J_{\text{HH}} = 7.2$ Hz) and -0.33 (2H, dd, Al(CHH)₂, $J_{\text{HH}} = 14$ Hz, $J_{\text{HH}} = 7.8$ Hz), -2.11 (1H, d, H¹, $J_{\text{HH}} = 6$ Hz), δ -4.00 (1H, dd, H², $J_{\text{HH}} = 10$ Hz, $J_{\text{HH}} = 3.7$ Hz). Isobutene: δ 4.69 (s, 2H, CH₂), 1.60 (s, 6H, Me). ^{13}C NMR (75.47 MHz, toluene- d_8 , 1,2-difluorobenzene, 20 °C): δ 107.4 (1C, C-H (Cp)), 32.4 (2C, Al(CH₂)₂, $J^1_{\text{CH}} = 139$ Hz), 14.5 (1C, Cp-CH₃, $J^1_{\text{CH}} = 129$ Hz).

C₂H₄(Flu)(5,6-C₃H₆-2-MeInd)Hf(Cl)CH₂SiMe₃ (12). C₂H₄(2-Me-5,6-(C₃H₆)Ind)HfCl₂ (0.75 g, 1.23 mmol) was suspended in 25 mL of toluene at room temperature. Me₃SiCH₂MgCl (6.6 mmol, 6.2 mL, 1.06 M in diethyl ether) was added to the suspension and the reaction mixture warmed to 80 °C for 26 h. The solvents were removed under vacuum. The product was extracted with a solvent mixture comprising 10 mL of toluene and 10 mL of light petroleum. Cooling the resulting solution to -25 °C for one week yielded small yellow crystals suitable for X-ray crystallography (0.4 g, 0.61 mmol, 50%). Anal. Calcd for C₃₂H₃₅ClHfSi: C, 58.09; H, 5.33. Found: C, 58.49; H, 4.83. ^1H NMR (300.13 MHz, CDCl₃, 25 °C): δ 7.89–7.79 (m, 3H, Ar), 7.49 (br, 2H, Ar), 7.34–7.25 (m, 3H, Ar), 7.16 (br, 1H, Ar), 7.00–6.95 (m, 1H, Ar), 5.73 (s, 1H, Cp-H), 4.28–4.16 (m, 1H, Al), 4.06–3.89 (m, 2H, Al), 3.76–3.67 (m, 1H, Al), 2.99–2.80 (m, 4H, Al), 2.25 (s, 3H, Cp-CH₃), 2.06–1.96 (m, 2H, Al), -0.33 (s, 9H, SiMe₃), -2.80 (d, 1H, $^2J = 12.4$ Hz, Hf-CHH), -2.95 (d, 1H, $^2J = 12.4$ Hz, Hf-CHH). ^{13}C NMR (75.47 MHz, CDCl₃, 25 °C): δ 143.81, 141.76, 127.76, 127.68, 127.35, 126.98, 126.67, 126.56, 124.05, 123.76, 123.35, 122.85, 122.34, 122.05, 121.30, 120.83, 119.02, 116.80, 114.49, 104.01 (‘Cp’), 96.89, 57.76 (Hf-CH₂), 32.31, 32.26, 28.42, 26.96, 26.44, 14.89 (Cp-CH₃), 2.01 (SiMe₃).

C₂H₄(Flu)(5,6-C₃H₆-2-MeInd)Hf(Me)CH₂SiMe₃ (13). To a suspension C₂H₄(Flu)(5,6-C₃H₆-2-MeInd)HfCl₂ (1.51 g, 2.48 mmol) in 25 mL of toluene was added Me₃SiCH₂MgCl (5.3 mmol, 5.0 mL, 1.06 M in diethyl ether) at room temperature. The reaction

mixture was heated to 80 °C for 12 h, during which time the suspended dichloride complex dissolved. The volatiles were removed under vacuum and the magnesium salts separated by extraction with a mixture of 20 mL of light petroleum and 20 mL of toluene. The resulting yellow solution was concentrated to approximately 20 mL under reduced pressure to remove the light petroleum. To this solution was added MeMgCl (2.5 mmol, 0.83 mL, 3 M in tetrahydrofuran) at room temperature and the reaction mixture stirred for 16 h. Removal of the volatiles gave a yellow oil, which solidified on addition of 20 mL of light petroleum. The addition of a further 20 mL of toluene was necessary to dissolve the product, and the insoluble residues were separated by filtration. The crude product crystallized from a yellow oil only after complete distillation of the solvent and was washed with 20 mL of light petroleum (0.9 g, 1.41 mmol, 57%). In order to prevent further losses, the compound was not recrystallized, and no elemental analysis was obtained. ^1H NMR (300.13 MHz, toluene- d_8 , 20 °C): δ 7.79 (dt, $J_{\text{HH}} = 8$ Hz, $J_{\text{HH}} = 1$ Hz, Ar), 7.75 (dt, $J_{\text{HH}} = 8$ Hz, $J_{\text{HH}} = 1$ Hz, Ar), 7.35–6.9 (overlapped with toluene), 6.77 (dd, $J_{\text{HH}} = 8.7$ Hz, $J_{\text{HH}} = 1$ Hz, Ar), 6.75 (dd, $J_{\text{HH}} = 8.7$ Hz, $J_{\text{HH}} = 1$ Hz, Ar), 5.84 (s, 1H, Cp-H), 3.77–3.26 (m), 2.93–2.62 (m), 1.92 (s, 3H, Cp-CH₃), -0.05 (s, 9H, SiMe₃), -1.24 (s, 3H, Hf-Me), -3.03 (m, 2H, diastereotopic Hf-CH₂). ^{13}C NMR (75.47 MHz, toluene- d_8 , 20 °C): δ 142.2, 140.8, 127.2, 124.1, 122.7, 122.5, 121.9, 119.3, 116.5, 103.4 (1C, C-H (Cp)), 95.6, 58.4 (1C, $J_{\text{CH}} = 106$ Hz, Hf-CH₂), 45.5 (1C, $J_{\text{CH}} = 115$ Hz, Hf-Me), 32.6, 32.5, 27.7, 26.9, 26.4, 25.2, 14.4 (1C, $J^1_{\text{CH}} = 127$ Hz, Cp-CH₃), 2.9 (3C, $J^1_{\text{CH}} = 116$ Hz, SiMe₃).

[C₂H₄(Flu)(5,6-C₃H₆-2-MeInd)HfCH₂SiMe₃]⁺[B(C₆F₅)₄]⁻ (14). In a glovebox, the appropriate amounts of C₂H₄(2-Me-5,6-(C₃H₆)Ind)Hf(Me)CH₂SiMe₃ (typically, 0.01–0.06 mmol) and CPh₃[B(C₆F₅)₃] (1.1 equiv) were placed in a 5 mm NMR tube capped with a rubber septum. Toluene- d_8 (0.5 mL) was added with appropriate cooling (<0 °C). After mixing the sample, the latter was allowed to stand until the phases had separated. The upper (organic) phase was removed; the oily phase was washed with 0.3 mL of toluene- d_8 and dissolved in 0.3 mL of toluene- d_8 and 0.1 mL of 1,2-difluorobenzene. A trace of SiMe₄ due to hydrolysis was observed. Since the compound is an equilibrium mixture of two diastereomers, the spectra are sensitive to the measurement temperature, so the NMR data are presented for -20 °C (slow exchange) and $+25$ °C (fast exchange).

^1H NMR (300.13 MHz, toluene- d_8 /1,2-difluorobenzene, -20 °C). Major isomer **14a**: δ 5.41 (s, 1H, Cp-H), 1.92 (d, 1H, $^2J_{\text{HH}} = 12.5$ Hz, Hf-CHH-Si), 1.63 (s, 3H, Cp-CH₃), 0.01 (s, 3H, SiMe), -0.18 (s, 3H, SiMe), -0.26 (d, 1H, $^2J_{\text{HH}} = 12.5$ Hz, Hf-CHH-Si), -2.58 (s, 3H, Hf-Me-Si). Minor isomer **14b**: δ 4.46 (s, 1H, Cp-H), 1.72 (s, 3H, Cp-CH₃), 0.16 (d, 1H, $^2J_{\text{HH}} = 12.5$ Hz, Hf-CHH-Si), -0.04 (s, 3H, SiMe), -0.14 (s, 3H, SiMe), -0.73 (d, 1H, $^2J_{\text{HH}} = 12.5$ Hz, Hf-CHH-Si), -1.58 (s, 3H, Hf-CH₃-Si). ^{13}C NMR (75.47 MHz, toluene- d_8 /1,2-difluorobenzene, -20 °C). Major isomer **14a**: δ 103.4 (1C, Cp-H), 102.9 (1C, Cp), 66.3 (1C, Hf-CH₂-Si), 19.0 (1C, Si-Me-Hf), 16.6 (1C, Cp-CH₃), -0.1 (1C, SiMe), -3.0 (1C, SiMe). Minor isomer **14b**: δ 102.0 (1C, Cp), 101.1 (1C, Cp-H), 16.5 (1C, Si-Me-Hf), 13.7 (1C, Cp-CH₃), 0.5 (1C, SiMe), -2.5 (1C, SiMe).

^1H NMR (300.13 MHz, toluene- d_8 /1,2-difluorobenzene, $+25$ °C): δ 5.25 (s, br, 1H, Cp-H), 1.77 (s, 3H, Cp-CH₃), -0.11 (d, 1H, $^2J_{\text{HH}} = 12.5$ Hz, Hf-CHH-Si), -0.71 (s, br, 9H, SiMe₃). One of the Hf-CHH-Si peaks not found (overlaps with other peaks). ^{13}C NMR (75.47 MHz, toluene- d_8 /1,2-difluorobenzene, $+25$ °C): δ 103.9 (2C, Cp-H and Cp), 72.7 (1C, CH₂), 68.9 (1C, CH₂), 32.6, 32.4, 29.2, 27.9, 26.4, 25.5, 14.5 (1C, SiMe₃).

X-ray Crystallography. Crystals of compound **12** are yellow plates. From a sample under oil, one, ca. $0.07 \times 0.04 \times 0.015$ mm, was mounted on a glass fiber and fixed in the cold nitrogen stream on a Bruker-Nonius diffractometer equipped with a FR591 rotating anode Mo K α radiation source ($\lambda(\text{Mo K}\alpha) = 0.71073$ Å)

and graphite monochromator. Intensity data were measured by thin-slice ω - and ϕ -scans with a Bruker-Nonius Roper CCD camera on a κ -goniostat. Total number of reflections recorded, to $\theta_{\max} = 25.0^\circ$, was 21 382, of which 4852 were unique ($R_{\text{int}} = 0.088$); 3784 were observed with $I > 2\sigma_I$.

Data were processed using the HKL software.⁴² The structure was determined by the direct methods routines in the SHELXS program⁴³ and refined by full-matrix least-squares methods, on F^2 's, in SHELXL.⁴³ The non-hydrogen atoms were refined with anisotropic thermal parameters. Hydrogen atoms were included in idealized positions, and their U_{iso} values were set to ride on the U_{eq} values of the parent carbon atoms. At the conclusion of the refinement, $wR_2 = 0.104$ and $R_1 = 0.084$ (2B) for all 4852 reflections weighted $w = 1/[\sigma^2(F_o^2) + 22.94P]$ where $P = (F_o^2 + 2F_c^2)/3$; for the observed data only, $R_1 = 0.054$. In the final difference map, the highest peak (ca. $1.27 \text{ e } \text{\AA}^{-3}$) was 0.96 \AA from Hf(1).

Scattering factors for neutral atoms were taken from the literature.⁴⁴ Computer programs used in this analysis have been noted above and were run through WinGX⁴⁵ on a Dell Optiplex 745 PC at the University of East Anglia.

(42) Programs: Standard Data Reduction using HKL (Denzo and Scalepack): (a) Otwinowski, Z.; Minor, W. Processing of X-ray diffraction data collected in oscillation mode. *Methods Enzymol.* **1997**, *276*, 307. (b) Absorption Correction: Sheldrick, G. M. *SADABS*, Version 2007/2; Bruker AXS Inc.: Madison, WI, 2007.

(43) Sheldrick, G. M. *Acta Crystallogr.* **2008**, *A64*, 112.

Crystal data: $\text{C}_{32}\text{H}_{35}\text{ClHfSi}$, $M = 661.6$, monoclinic, space group $P2_1/c$, $a = 17.2434(6) \text{ \AA}$, $b = 10.0370(3) \text{ \AA}$, $c = 17.8692(5) \text{ \AA}$, $\beta = 116.194(2)^\circ$, $V = 2775.06(15) \text{ \AA}^3$, $Z = 4$, $D_{\text{calc}} = 1.584 \text{ g cm}^{-3}$, $F(000) = 1320$, $T = 120(2) \text{ K}$, $\mu(\text{Mo K}\alpha) = 3.917 \text{ mm}^{-1}$.

Acknowledgment. We thank the Royal Society (grant 2006/R4 IJP) and RFBR (grant 06-03-32700) for the financial support of this work. We are grateful to Prof. Dr. Bernhard Rieger, TU Munich, for providing a sample of $\text{C}_2\text{H}_4(\text{Flu})(5,6\text{-C}_3\text{H}_6\text{-2-MeInd})\text{HfCl}_2$, to Dr. Louise Male (National X-ray Crystallography Service) for diffraction data collection on $\text{C}_2\text{H}_4(\text{Flu})(5,6\text{-C}_3\text{H}_6\text{-2-MeInd})\text{Hf}(\text{Cl})\text{CH}_2\text{SiMe}_3$, and to Dr. David L. Hughes (UEA) for assistance with the crystallographic analysis.

Supporting Information Available: NMR spectra of the intermediates; crystal and refinement data for $\text{C}_2\text{H}_4(\text{Flu})(5,6\text{-C}_3\text{H}_6\text{-2-MeInd})\text{Hf}(\text{Cl})\text{CH}_2\text{SiMe}_3$. Crystal data are also given as CIF files. This material is available free of charge via the Internet at <http://pubs.acs.org>.

OM800664P

(44) *International Tables for X-ray Crystallography*; Kluwer Academic Publishers: Dordrecht, 1992; Vol. C, pp 500, 219, and 193.

(45) Farrugia, L. J. *J. Appl. Crystallogr.* **1999**, *32*, 837.